Missouri University of Science and Technology
Scholars' Mine

NASA-Missouri Space Grant Consortium

Apr 21st, 3:15 PM - 4:15 PM

Computational Analysis of the HIFiRE-1 Hypersonic Test Model in ANSYS Fluent

Aidan Robert Murphy
Washington University in St. Louis

Follow this and additional works at: https://scholarsmine.mst.edu/nmsgc

Murphy, Aidan Robert, "Computational Analysis of the HIFiRE-1 Hypersonic Test Model in ANSYS Fluent" (2023). *NASA-Missouri Space Grant Consortium*. 20.
https://scholarsmine.mst.edu/nmsgc/2023/full-schedule/20

This Presentation is brought to you for free and open access by Scholars' Mine. It has been accepted for inclusion in NASA-Missouri Space Grant Consortium by an authorized administrator of Scholars' Mine. This work is protected by U. S. Copyright Law. Unauthorized use including reproduction for redistribution requires the permission of the copyright holder. For more information, please contact scholarsmine@mst.edu.

Computational Analysis of the HIFiRE-1 Hypersonic Test Model in ANSYS Fluent

Aidan Robert Murphy
Washington University in St. Louis
Dr. Ramesh K. Agarwal

Abstract

The Hypersonic International Flight Research Experimentation (HIFiRE) program explores and advances hypersonic aerospace systems by developing a multitude of test flight geometries and conducting experimental test flights to obtain data for use in validation of computational models and results. This study focuses on computational validation of heat flux, and calculation of static pressure profiles, skin friction coefficient profiles, and flow contours. The flow field studied is for Mach number 7.18 and an angle of attack (α) of 2°. The flow field include many compressible flow features such as an expansion wave at the intersection of the cone and flat cylindrical section, an oblique shock wave at the cylinder and flare connection point, and a detached bow shock at the tip of the geometry. These flow features are present in the experimental test flight data as well as in ground test studies conducted in the CALSPAN–University of Buffalo Research Center's LENS I facility along with computational results presented at the 2022 High-Fidelity CFD Workshop. Computations are performed using the Reynolds-Averaged Navier-Stokes (RANS) equations with one-equation Spalart-Allmaras (SA) turbulence model in ANSYS Fluent with suitable boundary conditions which give results for non-dimensionalized heat flux and static pressure profiles that closely match the computational results presented at the 2022 High-Fidelity CFD Workshop within 5% for $\alpha = 2°$.

Introduction

The Hypersonic International Flight Research Experimentation (HIFiRE) program consists of a multitude of flight tests that aim to explore and advance hypersonic aerospace systems. HIFiRE-1 was developed to obtain information about turbulent separated flow, boundary-layer transition, and shock wave/boundary-layer interaction in high-speed flow [1]. HIFiRE-1 has been adopted as one of the test cases for the High-Fidelity CFD Workshop organized by the NASA Langley Research Center in association with AIAA SciTech Forum in January 2022. This test case explores the steady state CFD modeling of the HIFiRE-1 geometry in hypersonic flow at $\alpha = 2°$ to evaluate the ability of different flow solvers to converge to the same solution when the mesh is refined [2]. The HIFiRE-1 geometry consists of an axisymmetric slightly blunt nose with 7° cone attached to a flat cylindrical section followed by a flare at 33° and ending with a smaller flat cylindrical section. Figure 1 shows this geometry as an axisymmetric half section of the full geometry.

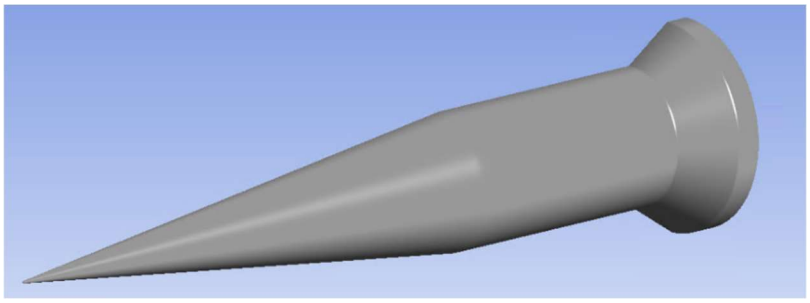

Figure 1: HIFiRE-1 geometry.

The HIFiRE-1 flight geometry dimensions are given in Fig. 2. Note that the labelled relevant dimensions differ slightly from Fig. 2 near the flare section (including the location and angle of the flare) since there were additional manufactured blunted noses and flare sections that could be added to change the overall geometry during testing [1].

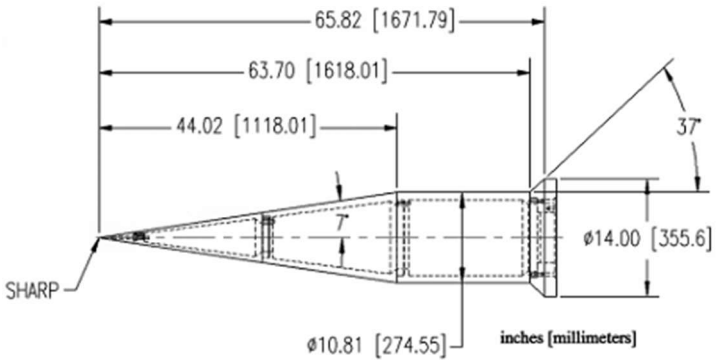

Figure 2: HIFiRE-1 geometry with relevant dimensions in imperial and metric units [1].

The HIFiRE-1 project is of great interest since there are plentiful resources for in-flight data collection as well as computational results that explore different areas of this hypersonic flow problem. Further analysis of hypersonic flow fields allows for a deeper understanding of the geometric impact of flow induced heat flux on the body. The ongoing joint efforts of this type of analysis (both experimental and computational) will aid in expanding the current hypersonic aerospace systems' knowledge base. Not only have these advancements taken place with the HIFiRE-1 geometry, but the whole HIFiRE program provides a deeper understanding of the practicalities of hypersonic flight. Experimental flight test results for the HIFiRE-1 program have been published in the AIAA Journal of Spacecraft and Rockets which provide detailed heating and pressure data over the full-scale HIFiRE-1 flight geometry. The goal of HIFiRE-1 experiment was to collect accurate flight data that can be utilized by CFD codes for validation of boundary-layer transition, turbulent separated flow, and shock/boundary-layer interaction on the geometry [1]. The results have also been published to compare the experimental test flight data to the computational analyses using CFD codes and a parabolized stability equation code for analyzing the boundary layer transition. The published CFD results compare the flight test data at $\alpha = 0°$ for laminar heating, transition onset, turbulent heating, and separation on the turbulent flare [3]. The analysis in this paper focuses on CFD simulation results at $\alpha = 2°$, M = 7.18 and a freestream Reynolds number Re = 10.213 x 10^6 /m [2]. Simulations for this angle of attack for

the HIFiRE-1 geometry are conducted to obtain results that can be compared to the computational results from the 2022 High-Fidelity CFD Workshop. This flow field corresponds to the same flow conditions dictated by the High-Fidelity CFD Workshop [2].

Computational Mesh

As part of the High-Fidelity CFD Workshop, there are multiple structured and unstructured grids given for the HIFiRE-1 geometry which include meshes for the overall geometry and individual meshes for the cone section [2]. An example of the provided structured mesh for the full geometry employed in the present computational analysis is a mesh around a three-dimensional cross-section along the x-y plane as shown in Fig. 3. The provided cgns mesh file was imported into ANSYS ICEM CFD [4]. Each full geometry mesh has flow domain elements and elements with labels for the inlet, outlet, symmetry plane, and the wall (i.e., the surface geometry of HIFiRE-1). In Fig. 3, the exterior red portion is the inlet domain, the orange region on the right is the outlet, the green elements correspond to the wall, the blue portion is the symmetry plane, and the purple elements in the interior of the mesh are the flow domain elements. The flow domain consists of hexahedron elements with 8 vertices, while the labeled exterior domains of the mesh consist of quadrilateral elements with 4 vertices.

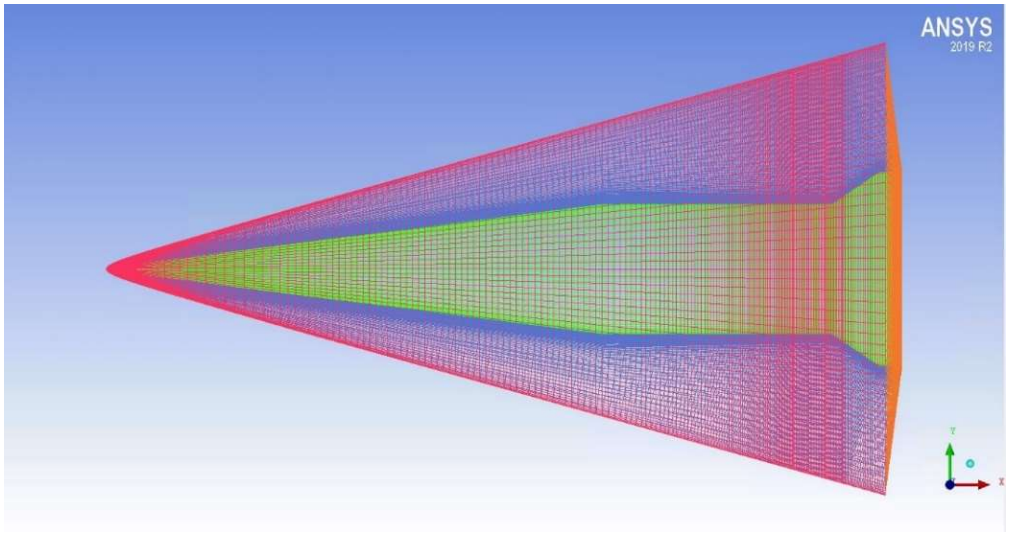

Figure 3: 3D cross-section grid on the surface and around the full HIFiRE-1 geometry.

Similar meshes were provided and imported into ICEM for the finer mesh sizes. The full geometry meshes consisted of coarse (3L), medium (2L), and fine (1L) grid refinements. Note that the distinction of the numbers (from 3 to 1), followed by "L," are the dictated abbreviations provided with the cgns files for the mesh. Table 1 displays some of the important mesh information for each of the three full geometry meshes.

Table 1: HIFiRE-1 full geometry mesh information and elemental breakdown.

		Coarse (3L)	Medium (2L)	Fine (1L)
Element Parts	Flow Domain	2,031,616	16,252,928	130,023,424
	Inlet	15,872	63,488	253,952
	Outlet	8,192	32,768	131,072
	Symmetry	65,536	262,144	1,048,576
	Wall	15,872	63,488	253,952
Summary	Total Elements	2,137,088	16,674,816	131,710,976
	Total Nodes	2,084,769	16,464,705	130,868,865

Numerical Method and Boundary Conditions

A density-based solver in ANSYS Fluent was used for all CFD simulations along with the energy equation. The case studied has a free stream Mach number of 7.18 at an operating pressure of 0 Pascals with an angle of attack of 2°. According to the 2022 High-Fidelity CFD Workshop, boundary conditions are to be set based on the type of the solver [2]. The inlet boundary condition was set as a velocity inlet with the following component velocities accounting for α = 2°: V_x = 2580.667 m/s and V_y = 90.119 m/s. The wall was set as an isothermal non-slip wall with T_w = 411.7229 K based on the wall temperature ratio of $\frac{T_w}{T_\infty}$ = 1.279 and T_∞ = 321.91 K. The outlet boundary condition was set as a pressure outlet at P_{outlet} = 6480 Pa. The spatial discretization of the solver had the following settings at start of the simulation: Green-Gauss node-based gradient, first- order-upwind scheme for the flow, and first-order upwind scheme for the modified turbulent viscosity. The solution utilized implicit formulation with a Roe-FDS flux-type. The numerical methods were further controlled with a 0.25 relaxation factor and a 0.5 Courant number. After a sufficient time throughout the solution process, the schemes for flow and modified turbulent viscosity were both switched to second order upwind. The turbulence model utilized in the simulations is described below:

Spalart-Allmaras (SA) Turbulence Model

A widely utilized turbulence model for many aerodynamic flows is the one-equation Spalart-Allmaras (SA) turbulence model. This turbulence model utilizes a single transport equation for the turbulent eddy viscosity. This model can be utilized for shock-induced separation, which is important for the HIFiRE-1 computational simulations since shock-induced separation is expected to occur. The SA model can also be used for the following conditions for compressible flow with heat transfer: A perfect gas assumption with Pr = 0.72, Pr_t = 0.90, and Sutherland's law for dynamic viscosity [5]. For this analysis, the fluid is air with modified parameters based on the previously mentioned conditions set forth for the SA model since the HIFiRE-1 flow-field is hypersonic, and hence compressible with heat transfer. It has been shown that the SA model can accurately predict shock-induced separation and responds to steep pressure gradients; however, there are difficulties in the ability of the model to compute post-shock reattachment in adverse pressure gradients [6]. The one-equation SA model is given by Eq. (1) in the non-conservation form as [5]:

$$\frac{\partial \hat{\nu}}{\partial t} + u_j \frac{\partial \hat{\nu}}{\partial x_j} = c_{b1}(1 - f_{t2})\hat{S}\hat{\nu} - \left[c_{w1} f_w - \frac{c_{b1}}{\kappa^2} f_{t2}\right]\left(\frac{\hat{\nu}}{d}\right)^2 + \frac{1}{\sigma}\left[\frac{\partial}{\partial x_j}\left((\nu + \hat{\nu})\frac{\partial \hat{\nu}}{\partial x_j}\right) + c_{b2}\frac{\partial \hat{\nu}}{\partial x_j}\frac{\partial \hat{\nu}}{\partial x_j}\right] \quad (1)$$

where $\hat{\nu}$ denotes the turbulent kinematic viscosity. The details of the SA model can be found in Refs. [5] and [6].

Results

Computational analysis was conducted in ANSYS Fluent for the HIFiRE-1 full geometry at α = 2° with M = 7.18 using an energy equation enabled density-based solver employing the Reynolds-Averaged Navier-Stokes (RANS) equations with the SA one-equation turbulence model. For a baseline computational comparison, the results from the 2022 High-Fidelity CFD workshop are utilized to compare the present computations in numerical values and overall trends with those of participants in the workshop. The workshop results consist of computational results from various organizations using different codes [7].

Pressure Distribution

In Figure 4, comparisons are made between the present computational analysis and the computational results from the workshop for the non-dimensionalized pressure (obtained dividing by P_∞). Figure 4 summarizes the normalized pressure results on leeward side, windward side, and in symmetry plane of HIFiRE-1 at 2° angle of attack on multiple meshes from MetaComp, Langley Research Center (LaRC), and Sandia National Lab. (SNL) [7]. In Fig. 4, the leeward pressure corresponds to the normalized pressure on surface of the wall along the intersection of the wall and the symmetry plane on the lee side of the incoming freestream at 2° angle of attack, the windward pressure runs along the intersection of the wall and the symmetry plane on the windward side of the incoming freestream at 2° angle of attack, and the symmetry plane pressure correlates to the pressure along the intersection of the wall and the x-z plane (i.e. the location where the flow is symmetric on either side of the geometry).

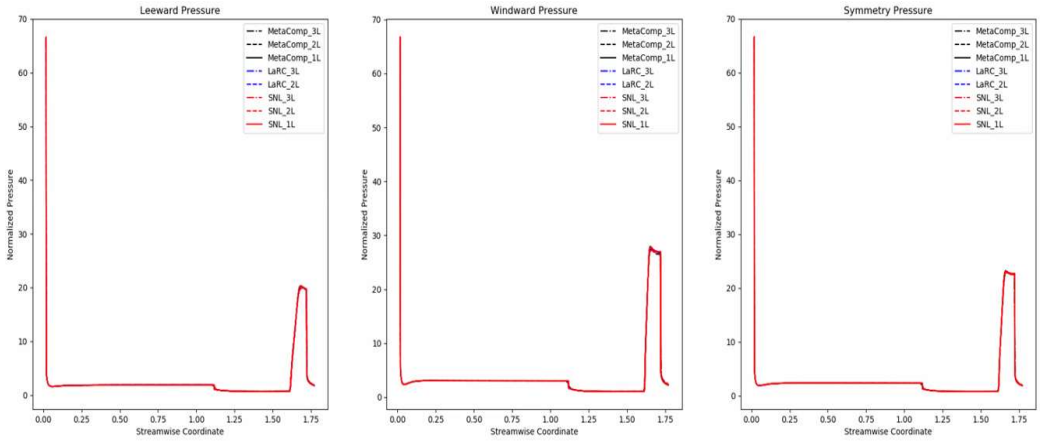

Figure 4: Computed non-dimensionalized pressure on leeward side, windward side and in symmetry plane of HIFiRE-1 at 2° angle of attack performed by three different organizations (MetaComp, LaRC and SNL) on multiple meshes [7].

The results of present computations for the non-dimensionalized pressure on leeward side, windward side, and symmetry plane of HIFiRE-1 are shown in Fig. 5. The overall non-dimensionalized pressure profiles between the workshop results (Fig. 4) and the present computational simulation results (Fig. 5) have a similar profile and are of similar magnitudes. It should be noted that in Fig. 5, computations are shown on each of the three provided meshes and they are nearly identical.

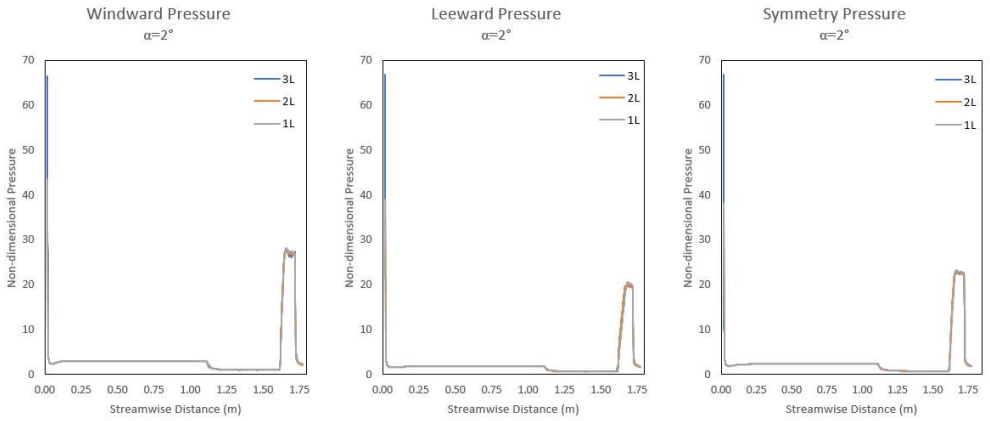

Figure 5: Present computations of non-dimensionalized pressure on leeward side, windward side and in symmetry plane of HIFiRE-1 at 2° angle of attack.

To further compare the present computed solutions at $\alpha = 2°$, we zoom into specific locations on the geometry and compare our normalized pressure results from the workshop participant results from MetaComp, LaRC and SNL. Figure 6 shows the pressure profiles obtained from the three workshop participants for the flare section of the HIFiRE-1 full geometry (from 1.5 m to 1.77 m). It should be noted that the non-dimensionalized static pressure is clearly much higher on the windward side than on the leeward side as expected. The overall pressure profile also corresponds to an increase in pressure as the geometry transitions into the flare section, and as the flare levels out at the end of the geometry the pressure profiles show a sharp decrease in pressure. Similar features in the pressure profiles are in the present results shown in Fig. 7 and are of similar magnitude.

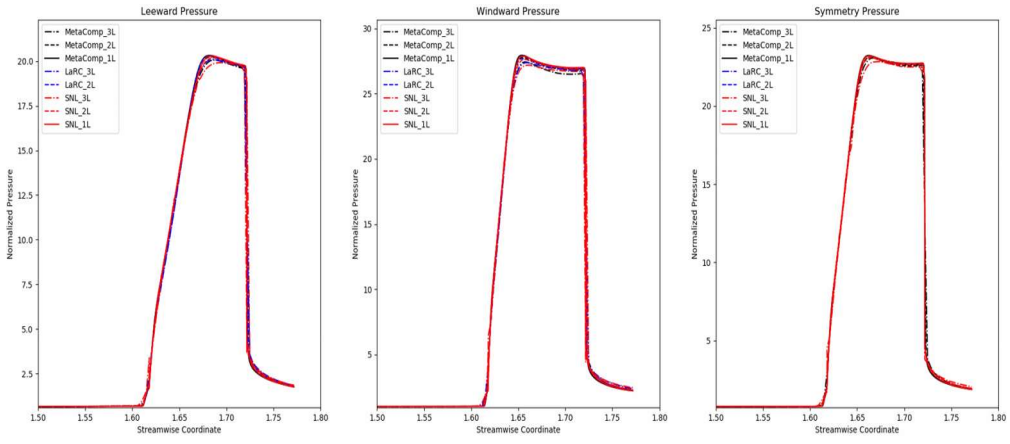

Figure 6: Zoomed-in non-dimensionalized pressure profiles in the flare region obtained by MetaComp, LaRC and SNL.

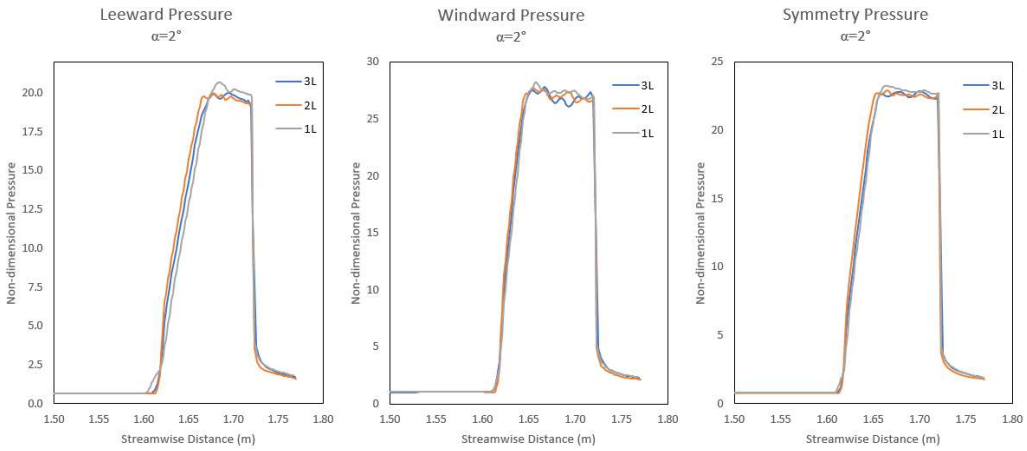

Figure 7: Present results for the zoomed-in non-dimensionalized pressure profiles in the flare region on all three meshes.

It can be noted from Fig. 6 and Fig. 7 that the shape and magnitude of the normalized pressure profiles are consistent in present computations with those of the workshop participants in the 2022 High-Fidelity CFD workshop. In Fig. 7, there is some notable instability in peak portion of these pressure profiles; it is likely due to the sharp increase in pressure at this section causing the numerical scheme to become slightly unstable for the number of iterations employed in obtaining the computed solution. This problem would be rectified if the solution is carried out to a larger number of iterations along with further mesh refinement in that area. It is seen from present computations on the finest mesh (1L) that most of the instability at the flare peak is resolved due to the refined mesh.

Heat Flux Distribution

The most important quantity of interest in any hypersonic flow simulation is the heat flux along the wall of the geometry. The heat flux is of great importance due to the large buildup of heat on the wall of a structure in a hypersonic freestream. Along with the non-dimensionalized pressure profiles given above, non-dimensionalized heat flux profiles were computed. The heat flux results were non-dimensionalized by $\frac{\kappa_\infty T_\infty}{r}$, where r is the radius of the cylindrical section of the HIFiRE-1 geometry. Figure 8 shows the computed non-dimensionalized heat flux profiles on the leeward side, windward side, and symmetry plane of HiFIRE-1 on each of the three provided meshes. The solutions for these three meshes are close to each other except for some minor differences in the peak heat flux region.

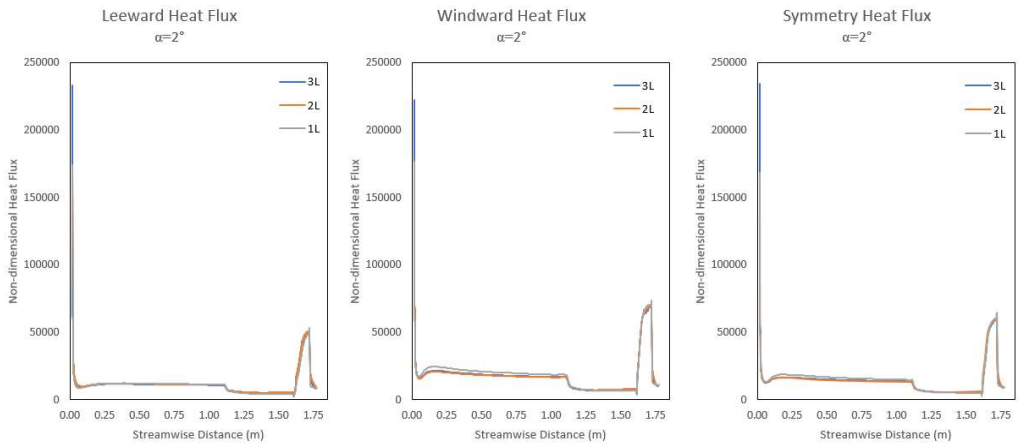

Figure 8: Present computations of non-dimensionalized wall heat flux along leeward side, windward side, and symmetry plane on each of the three meshes.

The overall variation and trend in the heat flux profiles is similar to that of the pressure profiles, but there are key differences especially near the flare section of the geometry where the heat flux is largest (not considering the stagnation region at the front tip of the geometry). The flare region, starting at ~1.6 m and extending to nearly the end of the geometry, has a steep but gradual increase in the heat flux until the flare section levels off. At that point the heat flux is at its largest peak value and then has a rapid decrease until the end of the geometry. Figure 9 shows the zoomed-in profiles of the computed normalized heat flux in flare region. Figure 10 shows the zoomed-in profiles of the normalized heat flux that were obtained from the 2022 High-Fidelity CFD Workshop. These profiles have the same trend as well as magnitudes within 5% as Fig. 9 leading to further affirmation that the present simulation results are consistent with the workshop results from three different investigators. Again, there is some instability that shows some waviness in the upper part of the profiles, but the overall results are consistent in shape and magnitude with the results of other participants from the workshop. Another important takeaway from these results is that as the mesh is refined from 3L to 1L, the curve is slightly less smooth, but all the important flow features are captured by each mesh.

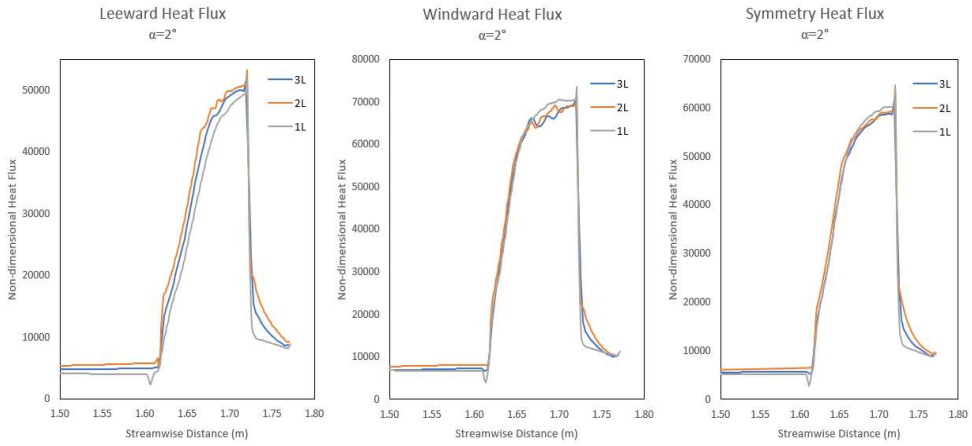

Figure 9: Present computed results for zoomed-in non-dimensionalized wall heat flux at the flare section on each of the three provided meshes.

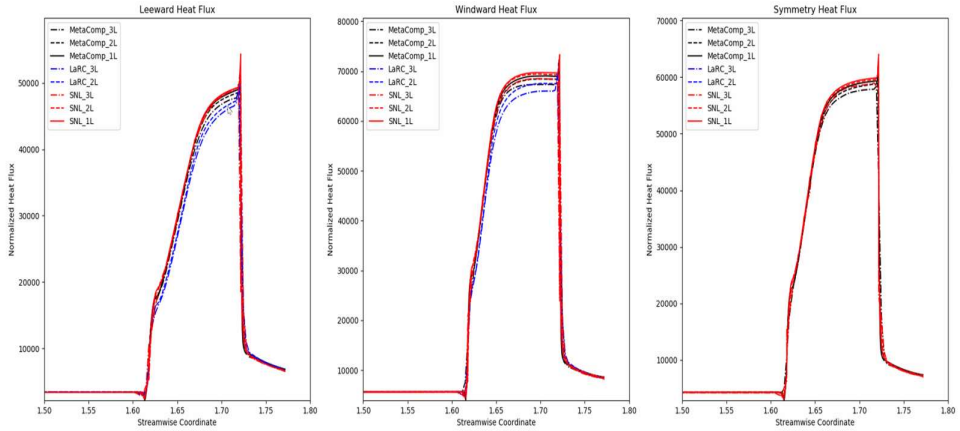

Figure 10: Zoomed-in non-dimensionalized wall heat flux at the flare section obtained from three workshop participants (MetaComp, LaRC and SNL) on various meshes.

Skin-Friction Distribution

In addition to heat flux, another quantity of interest is the skin-friction C_f along the surface of the body. The workshop did not focus on the profiles of C_f, but this is an important quantity in hypersonic flow since it relates to surface shear stress within the boundary layer in various flow regimes of the hypersonic body. This is particularly important since it also correlates with the overall heat transfer to the wall. Figure 11 displays the computed skin friction coefficient profiles along the leeward side, windward side, and the line of flow symmetry. The C_f profiles follow the same general trend as the heat flux profiles, but the peak is much more prominent near the flare section where there is also largest change in heat flux. At the onset of the flare there is a steep drop in the C_f values and after the decrease, there is the rapid and smooth increase as seen in the heat flux profiles (Figs. 9 and 10).

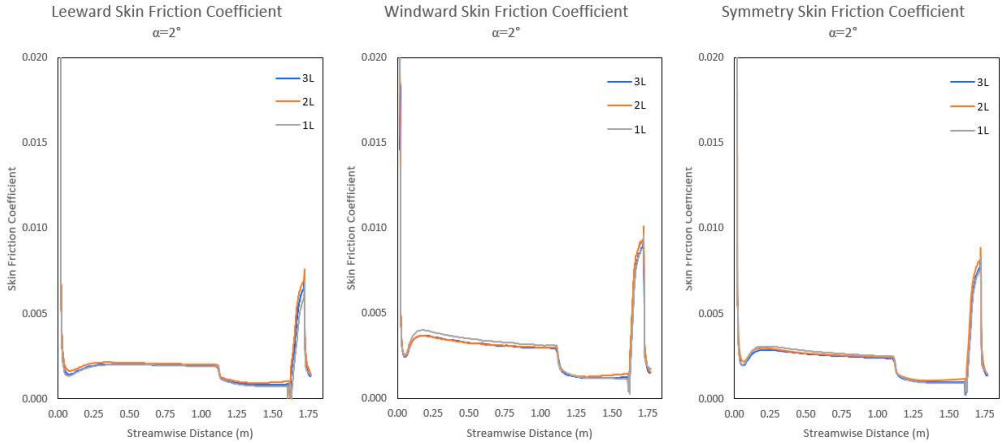

Figure 11: Computational results for the skin friction coefficient on all three provided meshes.

Apart from the very small instabilities in the profiles of non-dimensionalized pressure and heat flux, the present computed results overall are within 5% of the results obtained from the 2022 High-Fidelity CFD workshop. This shows that the present simulations are consistent and compare well in accuracy with the results of other workshop participants for HIFiRE-1 for the same flow conditions of $M = 7.18$ and $\alpha = 2°$ [2].

Conclusions

CFD simulations for the HIFiRE-1 geometry have been conducted using the Reynold-Averaged Navier-Stokes (RANS) equations with one-equation Spalart-Allmaras (SA) turbulence model in ANSYS Fluent to simulate the hypersonic flow field at Mach 7.18 and an angle of attack $\alpha = 2°$. The simulations show that the present numerical results are accurate when comparing the results for non-dimensionalized pressure and heat flux profiles with those reported in the 2022 High-Fidelity CFD Workshop for the $\alpha = 2°$ case. The computational results are within 5% of the results reported in the workshop by other investigators from MetaComp, NASA Langley Research Center and Sandia National Lab. The results follow the same general trend for each of the three provided meshes. Numerical results for the skin-friction, C_f, profiles are also provided as they serve to provide necessary information about the wall surface shear stress within the boundary layer. Skin-friction profiles have not been reported by the workshop; they can be helpful to other investigators interested in computing this flow.

Future Direction

Further hypersonic flow computations of NASA benchmark cases including Blottner Sphere, Flat Plate/Compression Corner, and CUBRC test cases of a blunt cone and bicone. Development of turbulent and transition models for hypersonic flows and their validation, with the inclusion of density variance equation and compressibility correction. Application of Machine Learning and Artificial Neural Net (ANN) to obtain accurate heat flux on relatively coarser grids. Evaluate the difficulty in computing hypersonic flow with cold adiabatic walls (compared to free stream) and propose solutions. Apply the above developed fundamental technology to compute hypersonic flow past space capsules such as Apollo and scramjet missiles. This investigation served to provide insight into the methods needed to properly simulate and produce accurate results for a steady hypersonic flow problem over a complex geometry.

Acknowledgement

Funding for this project was provided by NASA Missouri Space Grant Consortium Grant Award number 80NSSC20M0100.

Biography

Aidan Murphy is a second year PhD student at Washington University in Saint Louis, Missouri as a Dean's Select PhD Fellow. Aidan is originally from Beloit, Wisconsin. He has a Bachelor of Arts degree from Beloit College, and a Bachelor of Science degree in Mechanical Engineering from Washington University in Saint Louis. His research in CFD focuses on simulating and modeling complex flow phenomena in the field of hypersonics. Aidan hopes to pursue a career in hypersonic vehicle design and optimization using CFD.

References

1. Wadhams, T. P., Mundy, E., MacLean, M. G., and Holden, M. S., "Ground Test Studies of the HIFiRE-1 Transition Experiment Part 1: Experimental Results," Journal of Spacecraft and Rockets, Vol. 45, No. 6, 2008, pp. 1134–1148. https://doi.org/10.2514/1.38338.
2. Fisher, T., "High Fidelity CFD Workshop 2021: High Speed Steady Challenge Case: Hi-Fire 1," NASA Langley Research Center Turbulence Modeling Resource, 2021. URL:

https://turbmodels.larc.nasa.gov/Highfidelitycfd2021/SteadySupHypersonic_hifire_HFW_2021.pdf.
3. MacLean, M., Wadhams, T., Holden, M., and Johnson, H., "Ground Test Studies of the HIFiRE-1 Transition Experiment Part 2: Computational Analysis," Journal of Spacecraft and Rockets, Vol. 45, No. 6, 2008, pp. 1149–1164. https://doi.org/10.2514/1.37693.
4. "Index of /HFW2022/HiFire1/Pointwise," Massachusetts Institute of Technology Aerospace Computational Design Laboratory, 2021, Cambridge, MA. URL: https://acdl.mit.edu/HFW2022/HiFire1/Pointwise/.
5. Rumsey, C., "The Spalart-Allmaras Turbulence Model," NASA Langley Research Center Turbulence Modeling Resource, 2022. UR: https://turbmodels.larc.nasa.gov/spalart.html#sa.
6. Spalart, P. R., and Allmaras, S. R., "A One-Equation Turbulence Model for Aerodynamic Flows," AIAA Conference Paper AIAA-92-0439, 30th Aerospace Sciences Meeting and Exhibit, Reno, NV, 1992. https://doi.org/10.2514/6.1992-439.
7. Rumsey, C., and Wukie, N., "High Fidelity CFD Workshop 2022," NASA Langley Research Center Turbulence Modeling Resource, 2022. URL: https://turbmodels.larc.nasa.gov/highfidelitycfd_workshop2022.html.